

THE EFFECT OF HALIDE IONS ON THE ACTIVITY OF *d*-METAL COMPLEXES SUPPORTED ON NATURAL BENTONITE IN THE REACTION OF LOW TEMPERATURE OZONE DECOMPOSITION

Tatyana Rakitskaya^{ID}, Alla Truba^{ID}*, Ganna Dzhyga^{ID}

Faculty of Chemistry and Pharmacy, Odessa I.I. Mechnikov National University,
2, Dvoryanskaya str., Odessa, 65082, Ukraine
*e-mail: truba@onu.edu.ua

Abstract. The effect of halide ions (X= Cl⁻, Br⁻, I⁻) on the kinetics of ozone decomposition by compositions supported on the natural bentonite of the Dashukovske deposit in Ukraine (N-Bent(D)) has been studied. It was shown that the activity of the KX/N-Bent(D) composition in the ozone decomposition reaction increases in the series KCl<<KBr<KI, but the complex composition K₂PdCl₄-Cu(NO₃)₂-KX/N-Bent(D) demonstrates the maximum catalytic activity in the decomposition reaction in the presence of bromide ions. When the initial ozone concentration varied in the ozone-air mixture from 100 to 400 mg/m³, the reaction was first order for ozone at the beginning of the reaction (the first 10-15 min). The reaction order decreased in the stationary mode, which confirms the radical-chain reaction mechanism. It is shown that the bimetal composition K₂PdCl₄-Cu(NO₃)₂-KBr/N-Bent(D) demonstrates the longest protective action time (1800 min) at ozone concentration of 1 mg/m³.

Keywords: ozone, complex, catalytic activity, halide ion, natural bentonite.

Received: 08 November 2021/ Revised final: 03 June 2022/ Accepted: 09 June 2022

Introduction

The use of ozone as an oxidizing agent is associated with certain difficulties: its utilization rate is low at a relatively high cost, so various catalysts are used in ozonation reactions to increase this characteristic [1,2]. But even in this case, the residual concentration of ozone may exceed the maximum permissible concentration (MPC), therefore thermal, reagent and catalytic methods are applied for its decomposition [3]. Publications over the past ten years indicate the superiority of catalytic methods of ozone decomposition in air, and the most active catalysts were complex compositions [4-6], which contain palladium, silver, manganese oxides of different crystalline structures. Also, high activity is shown by metal-complex compounds of Mn(II) and Co(II) that are fixed on different carriers [7-10].

Analysis of patent and literature sources [11-16] showed that information on the use of supported metal complex catalysts (SMCC) for low-temperature ozone decomposition is very limited. The one-component catalysts PdCl₂/Fe₂O₃ (or BaO) [12], Mn(II)/AC [13], CuCl₂/CFM [14], Cu(NO₃)₂ (or Mn(NO₃)₂)/CLI [15] and the two-component catalysts PdCl₂-CuCl₂

(or NiCl₂)/Al₂O₃ [11], Mn(II)-Ti(IV)/ceramics have been reported [16]. Decomposition of ozone to the maximum permissible concentration ($MPC_{O_3} = 0.1 \text{ mg/m}^3$ for the working zone) was provided by catalysts containing PdCl₂ [12], PdCl₂-CuCl₂ [11] and CuCl₂ [14] on appropriate carriers. The greatest time of protective action ($\tau_{MPC} = 60 \text{ h}$) was showed by the catalyst CuCl₂/CFM under the conditions: $C_{O_3}^{in} = 1.5 \text{ mg/m}^3$, linear rate of ozone-air mixture 2.5-4.4 cm/s, temperature 283-313 K. Given in patent sources [11-16] research results do not contain information about the kinetics of ozone decomposition, therefore, it is impossible to determine the effect of each component, including the carrier, on the kinetic and stoichiometric parameters of the reaction and the protective action of the compositions.

Despite their limited use, SMCC have advantages over other types of catalysts, such as variation of activity due to changes in the nature of the central atom (Meⁿ⁺), ligands (L) and carriers, relatively simple production technology (impregnation of the carrier with a catalytic solution and drying at a temperature not exceeding 373-383 K).

One of the disadvantages of the known catalysts for the ozone decomposition is the presence in their composition of expensive carriers [3,17,18]. In this regard, the search for natural materials, potential carriers of metal-complex catalysts for ozone decomposition, is an urgent task in the field of environmental catalysts. The data about implication of some natural aluminosilicates as carriers of metal-complex compounds are presented in [7,19], but information about the use of natural bentonites is very limited.

Natural and modified bentonites are widely used as acid catalysts or as supporting carriers for oxides and salts of *d*-metals used in reactions of organic synthesis [20], destruction of organic compounds [21] and for water purification from dyes and herbicides [22]. However, the use of natural and modified bentonite as carrier of redox catalysts involving toxic gaseous substances is limited. Only some studies present the results of the catalytic activity of bentonites modified with Pd(II) and Cu(II) ions in the oxidation reactions of carbon monoxide [23-25], sulphur dioxide [26] and ozone decomposition [27]. Compositions containing K_2PdCl_4 , $Cu(NO_3)_2$, KBr and the carrier N-Bent(D) have been reported as being effective in ozone decomposition [27], thus such compositions can be used to purify the air from ozone.

The aim of this work is to establish the influence of the halide ions nature, the ratio of components and concentrations on the kinetics of ozone decomposition and the protective properties of the catalytic compositions that are optimal in composition.

Experimental

Materials

The natural bentonite of the Dashukovske deposit, Ukraine (N-Bent (D)) (TU U 14.2-00223941-006:2010) with the following chemical composition (mass %): SiO_2 –52.23; Al_2O_3 –22.58; Fe_2O_3 –10.17; TiO_2 –1.44; CaO –11.15; MgO –1.94; Na_2O –0.26; K_2O –0.22; $SiO_2/Al_2O_3 = 2.31$ was used as a carrier of catalytic compositions for the decomposition of ozone. The specific surface area determined from water vapor adsorption for the N-Bent (D) sample was $202 \text{ m}^2/\text{g}$ [28].

Samples containing potassium halides (KX; X= Cl^- , Br^- , I^-) (Sigma-Aldrich, USA), palladium(II) salts (K_2PdCl_4) (Sigma-Aldrich, USA), copper(II) ($Cu(NO_3)_2$) (Merks, Germany) and bimetal Pd(II)–Cu(II)-compositions were obtained by impregnating natural bentonite with water-alcohol solution of the corresponding

components with a given content. The resulting wet samples were placed in a Petri dish and kept at a temperature of 25°C for 24 h, and then dried in air at 110°C to constant weight. The content of the components was calculated in mol of substance per 1 g of carrier (mol/g).

Instruments and methods

The X-ray powder diffraction analysis was carried out on a Siemens D500 diffractometer ($CuK\alpha$ radiation, $\lambda = 1.54178 \text{ \AA}$) with a secondary beam graphite monochromator (Siemens AG, Munich, Germany). For data recording, the samples crumbled in a porcelain mortar were placed into a glass cell with an enclosed volume of $2 \times 1 \times 0.1 \text{ cm}^3$. XRD patterns were measured in the angle range of $3^\circ < 2\theta < 70^\circ$ with the pitch of 0.03° and acquisition time of 60 s for each position.

The bentonite samples were also characterized by scanning electron microscopy (SEM) using a JEOL-JSM5410 scanning microscope with an AZtech Energy X-max 50 energy dispersive spectrometer (Japan). The accelerating voltage was 15 kV.

Analysis of FT-IR spectra in the range from 400 to 4000 cm^{-1} with a 4 cm^{-1} resolution was carried out using a Perkin Elmer FT-IR spectrometer (U.S.A.). A sample of 1 mg of the material and 200 mg of KBr were used to obtain the pellets compressed under pressure of 7 tons/cm^2 for 30 s [29].

The samples tested in the reaction of ozone decomposition were as follows: the ozone-air mixture (OAM), with a required ozone concentration was obtained with the help of an IG-1Sh ozonizer by a silent electric discharge action on air oxygen. An OAM feed was controlled based on rheometer readings. The corresponding sample (10 g) was placed into a gas-flow fixed-bed reactor and the OAM with RH of 65% at 20°C passed through the sample at a linear rate (u) of 4.2 cm/s . Ozone decomposition was monitored by the measuring of the final (outlet) ozone concentration, $C_{O_3}^f$. An initial ozone concentration, $C_{O_3}^{in}$, equal to 100 mg/m^3 was controlled by a Tsyclon-Reverse optical analyzer, whereas $C_{O_3}^f$ values were measured either by the Tsyclon-Reverse optical analyzer (detection limit of 1 mg/m^3) (“Optec“, Russia) or by a 652EKh04 electrochemical gas analyzer (detection limit of 0.01 mg/m^3) (“Analitpribor“, Ukraine) [30].

The reaction rate (W) calculations based on the data of ozone concentration changing after

OAM passing through the static bed of the catalyst were made using Eq.(1).

$$W = \frac{\omega(C_{O_3}^{in} - C_{O_3}^f)}{m_s}, \text{ mol/(g}\times\text{s)} \quad (1)$$

where, $\omega = 1.67 \times 10^{-2}$ is the OAM volume flow rate, L/s;

$C_{O_3}^{in}$ and $C_{O_3}^f$ are the initial and final ozone concentrations in the OAM, mol/L;
 m_s is the mass of the catalyst sample, g.

The reaction rate values measured after one minute of OAM passing, designated as the initial reaction rate, W_{in} , were used to characterize the process.

The reaction rate constant, $k_{1/2}$, was quantified for the half-conversion time, $\tau_{1/2}$, i.e. for the moment of time when the degree of ozone decomposition became equal to 50%, as follows to Eq.(2).

$$k_{1/2} = \frac{0.69}{\tau_{1/2}}, \text{ s}^{-1} \quad (2)$$

An activity of the samples was evaluated based on the following parameters:

- τ_{MPC} is the time of protective action, i.e. the period of time from the start of the experiment, during which $C_{O_3}^f < MPC_{O_3}$;
- $\tau_{1/2}$ is the half-conversion time, the period of time from the start of the experiment up to the moment when $C_{O_3}^f$ becomes equal to $0.5 C_{O_3}^{in}$;
- Q_{exp} is an experimental amount of O_3 moles, i.e. the amount of ozone entered into the reaction up to a moment of experiment termination and calculated as an area under the corresponding curve plotted as a ΔC_{O_3} vs. τ .

Results and discussion

XRD analysis

The diffraction patterns of N-Bent(D) samples and K_2PdCl_4 - $Cu(NO_3)_2$ -KBr/N-Bent(D) catalyst were obtained (Figure 1) and the montmorillonite phase (M) was identified in the composition of natural bentonite, for which 2θ and (d , Å) were determined: 5.739 (15.387), 19.743 (4.493), 35.830 (2.504), 61.710 (1.501); phases of α -quartz (Q) and calcite (C) were also identified. During the formation of the catalyst, no significant structural changes in the support occurred ($d_{006} = 1.501$ Å), and new phases didn't form in the catalyst components.

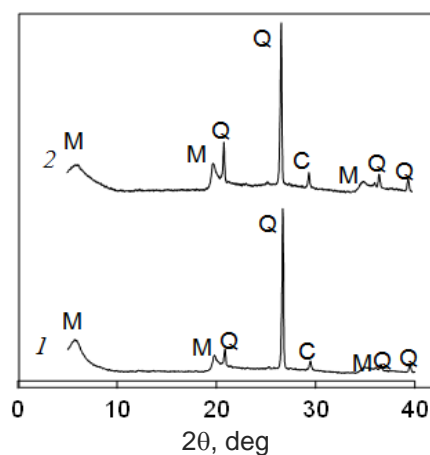


Figure 1. XRD patterns of natural bentonite N-Bent(D) (1) and catalyst Pd(II)-Cu(II)/N-Bent(D) (2).

Morphology

SEM images of samples N-Bent(D) (1) and catalyst Pd(II)-Cu(II)/N-Bent(D) are shown in Figure 2. It can be seen that natural bentonite (Figure 2(a) and (b)) consists of flake-like particles. The surface morphology practically does not change upon the deposition of catalyst components (Figure 2(c)), and also after reaction with ozone (not shown here).

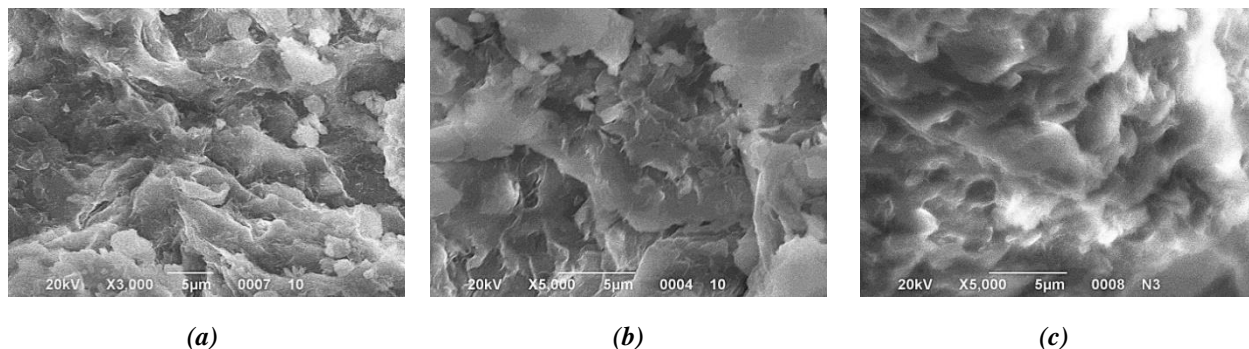


Figure 2. SEM images of natural bentonite N-Bent(D) (a) and (b) and catalyst Pd(II)-Cu(II)/N-Bent(D) (c).

FT-IR spectral investigation

The IR spectra of the N-Bent(D) samples and the Pd(II)–Cu(II)/N-Bent(D) catalyst (Figure 3, Table 1) reflect absorption bands characteristic of the main montmorillonite phase in the region of valence and deformation vibrations of structural groups, as well as absorption bands of α -quartz and calcite impurities [31]. The characteristic doublet at 798 and 779 cm^{-1} indicates the presence of the α - SiO_2 phase in the sample. The absorption band at 1421 cm^{-1} indicates that a calcite phase is present in the sample N-Bent(D); the high-frequency shift ($\Delta\nu = +9 \text{ cm}^{-1}$) during the deposition of catalyst components proves the formation of Pd(II) and Cu(II) carbonates [32].

Testing catalyst compositions in ozone decomposition reaction

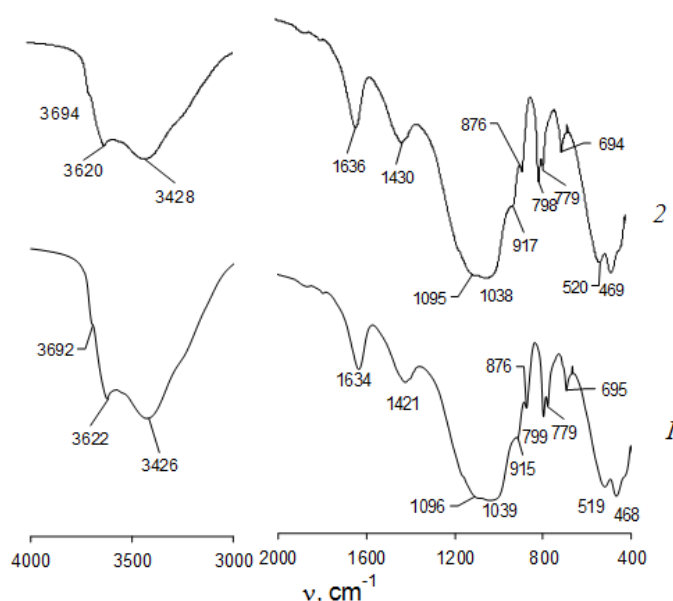
Composition $KX/N\text{-Bent}(D)$ ($X = \text{Cl}^-, \text{Br}^-, \text{I}^-$). Halide ions, both in solutions [33] and fixed

on porous carriers [18], except for the fluoride ion, which is characterized by a high redox potential $\varphi_{\text{F}_2/2\text{F}^-} = 2.87 \text{ V}$, are oxidized by ozone. Figure 4 shows the kinetic curves of the final concentration of ozone $C_{\text{O}_3}^f$ in time (τ) for natural bentonite under variation of halide ions content in the systems KCl/N-Bent(D) (Figure 4(a)), KBr/N-Bent(D) (Figure 4(b)), KI/Bent(D) (Figure 4(c)) from 0.1×10^{-4} to $3.0 \times 10^{-4} \text{ mol/g}$. It is seen that bentonite itself (curve 1, Figure 4(a)) decomposes ozone, but its activity is low: in the first minute of the reaction $C_{\text{O}_3}^f > 0.5 C_{\text{O}_3}^{\text{in}}$; within 50 min the final ozone concentration reaches the initial one. Decomposition of ozone by bentonite is explained by the fact that it contains Fe_2O_3 , Al_2O_3 and SiO_2 , and the greatest activity according to [34] is observed in Fe_2O_3 .

Table 1

Wavenumbers (cm^{-1}) for absorption maxima in FT-IR spectra of N-Bent(D) and Pd(II)-Cu(II)/N-Bent(D).

| Structural group | N-Bent(D) | | Pd(II)-Cu(II)/N-Bent(D) | |
|---|------------------------|---------------|-------------------------|---------------|
| | ν | δ | ν | δ |
| M–OH | 3692 sh | - | 3694 sh | - |
| Al–Al–OH | 3622 | 915 bend | 3620 | 917 bend |
| Al– Fe^{3+} –OH | - | 876 | - | 876 |
| H_2O | 3426 | 1634 | 3428 | 1636 |
| Si–O–Si (tetrahedron) | 1163 sh, 1096 sh, 1039 | 468 | 1165 sh, 1095 sh, 1038 | 469 |
| Si–O–Al | - | 519 | - | 520 |
| Si–O–Mg | - | 434 sh | - | 432 sh |
| α - SiO_2 (α -quartz) | - | 799, 779, 695 | - | 798, 779, 694 |
| CO_3^{2-} | - | 1421 | - | 1430 |

**Figure 3. FT-IR spectra of natural bentonite N-Bent(D) (1) and catalyst Pd(II)-Cu(II)/N-Bent(D) (2).**

The nature of the kinetic curves changes significantly when applied to natural bentonite halide ions. In the case of the composition KCl/N-Bent(D) (Figure 4(a)) the protective action time (τ_0) is absent, and the half-life of ozone ($\tau_{1/2}$) and the number of moles of unreacted ozone pass through the maximum at $C_{\text{KCl}} = 1.0 \times 10^{-4}$ mol/g.

The profiles of the kinetic curves change with varying C_{KBr} and C_{KI} ; areas appear where ozone is not detected at the reactor outlet, and the duration (τ_0) of this area increases with increasing C_{KBr} and C_{KI} . At the same time, τ_0 for the KI/Bent(D) composition is 6–10 times higher than τ_0 for the KBr/N-Bent(D) composition. The amount of ozone reacted during its half-conversion ($C_{\text{O}_3}^f = 0.5 C_{\text{O}_3}^{\text{in}}$) also increases with an increase in the KBr and KI content in the compositions; however, no proportional dependence is observed, which indicates a complex mechanism of ozone decomposition in the presence of halide ions.

Based on the data obtained, it can be concluded that the activity of the KX/N-Bent(D) compositions in the ozone decomposition reaction increases in the KCl \ll KBr $<$ KI series, which correlates with the enhancement of the reducing properties of halide ions.

The effect of the combined action of Pd(II), Cu(II) and halide ions. The peculiarity of catalytic ozone decomposition reactions is that they are usually carried out by a radical-chain mechanism.

The most effective catalysts are complex compounds of *d*-metals [7-10]. The case of the use of two metal-complex compounds may be a demonstration of synergistic, additive or inhibitory action. For ozone decomposition reactions, these effects have been scarcely studied, although it is known that for some metals and metal oxides such phenomena are observed [3]. According to [27], Cu(II) has an inhibitory effect on ozone decomposition by the catalytic composition $\text{K}_2\text{PdCl}_4\text{-Cu}(\text{NO}_3)_2\text{-KBr/N-Bent(D)}$. The nature of halide ions significantly affects the activity of monocomponent compositions KX/N-Bent(D) in the ozone decomposition reaction (Figure 4). In the presence of transition metal ions, the function of halide ions becomes more complicated. They not only interact with ozone, but also participate in the processes of complexation and reduction of metal ions. Halide ions form more stable complexes with Pd(II) than with Cu(II), and iodide ions are able to reduce Cu(II) to Cu(I) ($\varphi_{\text{I}_2/\text{I}^-} = 0.54$ V), so it is important to compare the influence of the nature of the halide ion on the kinetics of ozone decomposition in the presence of $\text{K}_2\text{PdCl}_4\text{-Cu}(\text{NO}_3)_2\text{-KX/N-Bent(D)}$ -composition. It is established (Figure 5) that due to the listed reasons the system containing bromide ions shows the greatest activity. A similar effect of bromide ions was found in the case of oxidation of CO by oxygen in the presence of Pd(II)-Cu(II)/ \bar{S} (\bar{S} – natural and acid-modified carriers) [25,35].

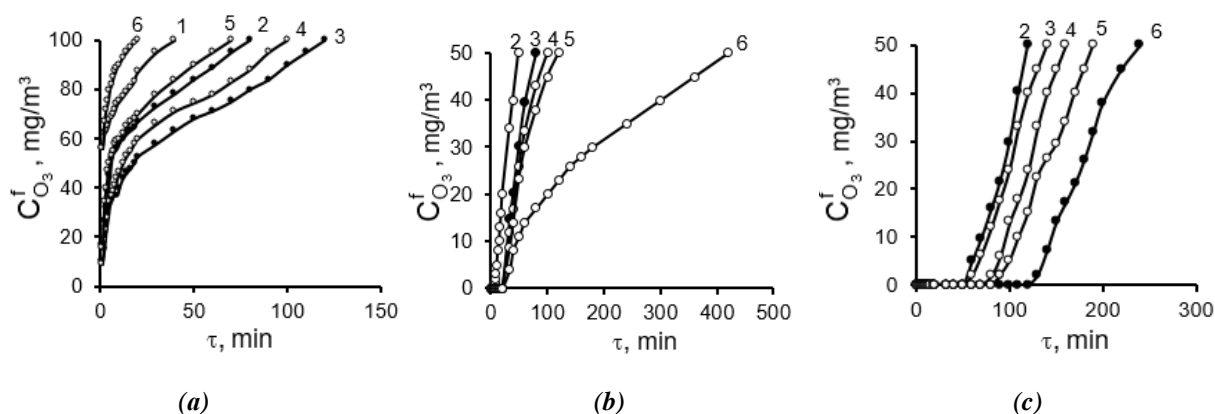


Figure 4. Time dependence of $C_{\text{O}_3}^f$ in ozone decomposition reaction at different halide-ions content

in the system KX/N-Bent(D) $C_{\text{KX}} \times 10^4$, mol/g: 1 – 0; 2 – 0.1; 3 – 1.0; 4 – 1.5; 5 – 2.0; 6 – 3.0.

($C_{\text{O}_3}^{\text{in}} = 100$ mg/m³; $u = 4.2$ cm/s; $m_s = 10$ g).

KX: KCl (a); KBr (b); KI (c)

The kinetic data (Figure 5) show that the stationary mode in ozone decomposition systems is not established at the indicated ratio of the components and experimental conditions. A change in the reaction kinetics is achieved by increasing the concentration of bromide ions and a long-term stationary mode is established already at $C_{KBr} = 3 \times 10^{-4}$ mol/g (Figure 6). Under these conditions, the ozone concentration in the ozone-air mixture was varied from 100 to 400 mg/m³ (Figure 7). The profile of the kinetic curves reflecting the change in the reaction rate (W) over time does not change with increasing $C_{O_3}^{in}$.

Figure 7 and data in Table 2 show that the initial reaction rate (W_{in}) calculated for the first minute of the experiment increases in proportion to the initial ozone concentration. At the same time, the proportional relationship is not observed in the stationary mode: the reaction rate increases by only 2.5 times with a 4-fold increase of $C_{O_3}^{in}$.

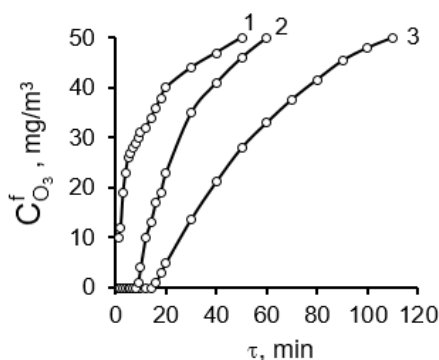


Figure 5. Time dependence of $C_{O_3}^f$ in ozone decomposition reaction by composition Pd(II)-Cu(II)-KX/N-Bent(D) at different KX: 1 – KCl; 2 – KBr; 3 – KI ($C_{Pd(II)} = 1.02 \times 10^{-5}$; $C_{Cu(II)} = 0.59 \times 10^{-5}$; $C_{KX} = 1.0 \times 10^{-4}$ mol/g; $C_{O_3}^{in} = 100$ mg/m³; $u = 4,2$ cm/s; $m_s = 10$ g).

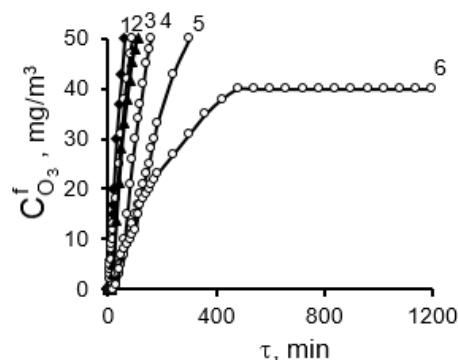


Figure 6. Time dependence of $C_{O_3}^f$ in ozone decomposition reaction at different contents of KBr in the system Pd(II)-Cu(II)-KBr/N-Bent(D) $C_{KBr} \times 10^4$, mol/g: 1 – 0; 2 – 0.1; 3 – 1.0; 4 – 1.5; 5 – 2.0; 6 – 3.0 ($C_{Pd(II)} = 1.02 \times 10^{-5}$ mol/g; $C_{Cu(II)} = 0.59 \times 10^{-5}$ mol/g; $C_{O_3}^{in} = 100$ mg/m³; $u = 4.2$ cm/s; $t = 20^\circ\text{C}$; $m_s = 10$ g).

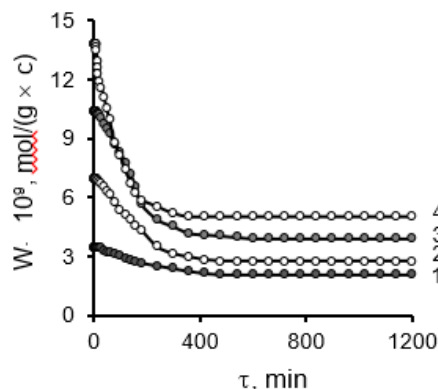


Figure 7. Time dependence of reaction rate in ozone decomposition reaction by system K_2PdCl_4 -Cu(NO₃)₂-KBr/N-Bent(D) at different $C_{O_3}^{in}$ (mg/m³) in ozone-air mixture: 1 – 100; 2 – 200; 3 – 300; 4 – 400 ($C_{Pd(II)} = 1.02 \times 10^{-5}$; $C_{Cu(II)} = 0.59 \times 10^{-5}$; $C_{KBr} = 3.0 \times 10^{-4}$ mol/g; $u = 4,2$ cm/s; $m_s = 10$ g).

Table 2

Effect of $C_{O_3}^{in}$ on kinetic and stoichiometric parameters of ozone decomposition reaction by composition K_2PdCl_4 -Cu(NO₃)₂-KBr/N-Bent(D).

| $C_{O_3}^{in}$, mg/m ³ | $W_{in} \times 10^9$, mol/(gxs) | $W_{st} \times 10^9$, mol/(gxs) | τ_0 , min | $\tau_{1/2}$, min | $k_{1/2} \times 10^4$, s ⁻¹ | $Q_{exp} \times 10^4$, mol O ₃ |
|------------------------------------|----------------------------------|----------------------------------|----------------|--------------------|---|--|
| 100 | 3.5 | 2.1 | 20 | -* | -* | 17.0 |
| 200 | 6.9 | 2.8 | 14 | 240 | 0.5 | 22.7 |
| 300 | 10.4 | 3.9 | 12 | 210 | 0.6 | 32.5 |
| 400 | 13.8 | 5.0 | 9 | 140 | 0.8 | 39.1 |

*Experiment was stopped at $C_{O_3}^f = 40$ mg/m³.

Experimental conditions: $C_{Pd(II)} = 1.02 \times 10^{-5}$; $C_{Cu(II)} = 0.59 \times 10^{-5}$; $C_{KBr} = 3.0 \times 10^{-4}$ mol/g; $u = 4.2$ cm/s; $m_s = 10$ g.

The order of the reaction is lowered; the reaction rate constant $k_{1/2}$, calculated from the half-life of ozone ($\tau_{1/2}$), is not a constant. The totality of the obtained data indicates a radical chain mechanism of ozone decomposition, which is consistent with numerous studies [3,9,18].

Protective properties of compositions against ozone. The protective properties of the compositions are characterized by the time during which the air is purified from ozone to a concentration below or equal to MPC, i.e. $C_{O_3}^f \leq MPC_{O_3}$. The kinetics study of ozone decomposition at $C_{O_3}^{in} = 100 \text{ mg/m}^3$ showed that each component of the $K_2PdCl_4-Cu(NO_3)_2-KBr/N-Bent(D)$ composition participates in the reaction with ozone.

The test results of individual compositions at $C_{O_3}^{in} = 1.0 \text{ mg/m}^3$ (10 MPC) are presented in Figure 8 and are summarized in Table 3. It can be

noticed that natural bentonite (curve 1) does not show protective properties against ozone: $C_{O_3}^f > MPC_{O_3}$ already in the first minute of transmission of the ozone-air mixture. In the case of KBr/N-Bent(D) and Cu(II)-KBr/N-Bent(D) compositions, the samples provide complete decomposition of ozone in only 18 and 30 min, respectively. Maximum activity (more than 20 h) is shown by mono- Pd(II) and bimetallic Pd(II)-Cu(II)-compositions in the presence of bromide ions: complete ozone decomposition is provided; the protective action time is 25 and 30 h, respectively. It should be noted that in both cases a stationary state is established with the final ozone concentration of 0.1 mg/m^3 .

To resolve the issue of composition application, for instance, in personal protective equipment for respiratory system, it is necessary to have data about the influence of the effective contact time of ozone-air mixture on the time of the protective action of the compositions.

Table 3

Kinetic and stoichiometric parameters of ozone decomposition reaction with mono- and bimetallic compositions.

| Compositions based on N-Bent(D) | τ_0 , min | τ_{MPC} , min | $C_{O_3}^f$, mg/m ³ | $Q_{exp} \times 10^6$, mol O ₃ |
|---------------------------------|----------------|--------------------|---------------------------------|--|
| N-Bent(D) | - | - | 1.0 | 0.9 |
| KBr | 18 | 30 | 0.1 | 0.4 |
| Cu(II)-KBr | 30 | 50 | 0.1 | 0.6 |
| Pd(II)-KBr | 1260 | 1500 | 0.1* | 33.6 |
| Pd(II)-Cu(II)-KBr | 1260 | 1800 | 0.1* | 37.6 |

* – the stationary mode is established.

Experimental conditions: $C_{Pd(II)} = 2.72 \times 10^{-5}$; $C_{Cu(II)} = 2.9 \times 10^{-5}$; $C_{KBr} = 1.02 \times 10^{-4} \text{ mol/g}$; $u = 4.2 \text{ cm/s}$; $m_s = 10 \text{ g}$.

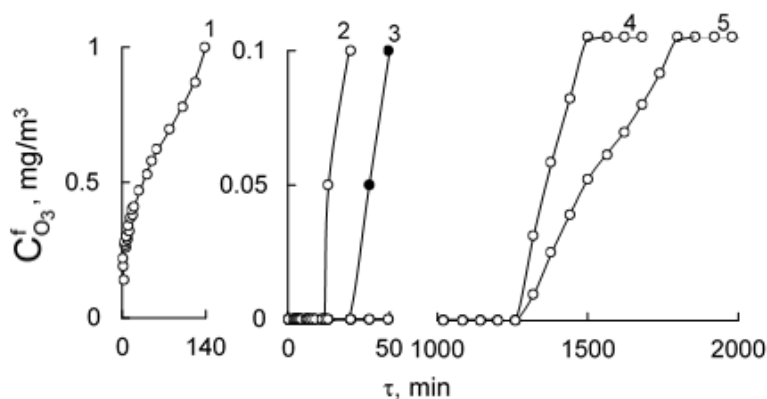


Figure 8. Time dependence of $C_{O_3}^f$ by ozone decomposition with samples: 1 – N-Bent(D); 2 – KBr/N-Bent(D);

3 – Cu(II)-KBr/N-Bent(D); 4 – Pd(II)-KBr/N-Bent(D); 5 – Pd(II)-Cu(II)-KBr/N-Bent(D)

($C_{Pd(II)} = 2.72 \times 10^{-5}$; $C_{Cu(II)} = 2.9 \times 10^{-5}$; $C_{KBr} = 1.02 \times 10^{-4} \text{ mol/g}$; $C_{O_3}^{in} = 1 \text{ mg/m}^3$; $u = 4.2 \text{ cm/s}$; $m_s = 10 \text{ g}$).

Different values of τ_{eff} were achieved by varying the sample weight (layer height at a constant linear rate of ozone-air mixture). Kinetic studies (Figure 9) showed that with an increase of τ_{eff} from 0.17 to 0.6 s, the time of protective action increases from 240 min to 1800 min, but the stationary decomposition of ozone at $C_{O_3}^f = MPC_{O_3}$ is achieved only at $\tau_{\text{eff}} = 0.6$ s.

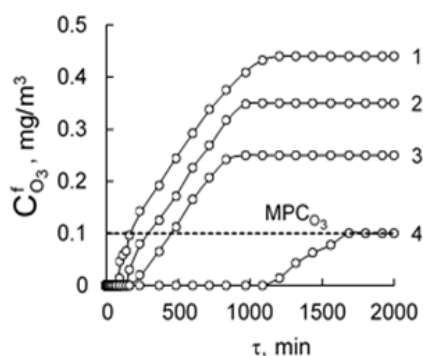


Figure 9. Time dependence of $C_{O_3}^f$ in ozone decomposition reactions with samples Pd(II)-Cu(II)-KBr/N-Bent(D) by various effective contact time τ_{eff} , s: 1 – 0.17; 2 – 0.31; 3 – 0.46; 4 – 0.60 ($C_{\text{Pd(II)}} = 2.72 \times 10^{-5}$; $C_{\text{Cu(II)}} = 2.9 \times 10^{-5}$; $C_{\text{KBr}} = 1.02 \times 10^{-4}$ mol/g; $C_{O_3}^{\text{in}} = 1$ mg/m³).

Conclusions

It is shown that the catalytic composition $K_2PdCl_4-Cu(NO_3)_2-KBr/N-Bent(D)$ decomposes ozone effectively at $C_{O_3}^{\text{in}}$ in the ozone-air mixture from 1 to 400 mg/m³. Ozone interacts with each component of the catalytic composition. It is shown that the activity of the KX/N-Bent(D) composition in the ozone decomposition reaction increases in the row $KCl \ll KBr < KI$, which correlates with an increase in their reducing properties (the redox potential of the $X_2/2X^-$ pair decreases). For the catalytic Pd(II)-Cu(II)-composition the maximum activity is observed in the presence of bromide ions. At $C_{\text{KBr}} = 3.0 \times 10^{-4}$ mol/g the catalytic composition decomposes ozone with the establishment of a stationary mode.

Each mono-component composition exhibits protective properties at $C_{O_3}^{\text{in}} = 1$ mg/m³, providing air purification below 0.1 mg/m³. However, the composition $K_2PdCl_4-Cu(NO_3)_2-KBr/N-Bent(D)$ showed the longest time of protective action (1800 min), while a constant ozone concentration at the MPC level is

maintained in the stationary mode for a long time. Such catalyst compositions can be recommended for applying in personal protective equipment for the respiratory system.

References

- Lin, F.; Wang, Z.; Ma, Q.; Yang, Y.; Whiddon, R.; Zhu, Y.; Cen, K. Catalytic deep oxidation of NO by ozone over MnOx loaded spherical alumina catalyst. *Applied Catalysis B: Environmental*, 2016, 198, pp.100–111. DOI: <https://doi.org/10.1016/j.apcatb.2016.05.058>
- Nawrocki, J.; Fijolek, L. Catalytic ozonation – Effect of carbon contaminants on the process of ozone decomposition. *Applied Catalysis B: Environmental*, 2013, 142-143, pp. 307–314. DOI: <https://doi.org/10.1016/j.apcatb.2013.05.028>
- Rakitskaya, T.; Truba, A.; Ennan, A. Ozon. Physicochemical Properties and Catalytic Decomposition Methods. Astroprint: Odessa, 2020, 223 p. (in Russian). <https://www.astroprint.ua/>
- Ren, C.; Zhou, L.; Shang, H.; Chen, Y. Effect of preparation method on the performance of Pd-MnOx/ γ -Al₂O₃ monolithic catalysts for ground-level O₃ decomposition. *Chinese Journal of Catalysis*, 2014, 35(11), pp. 1883–1890. DOI: [https://doi.org/10.1016/S1872-2067\(14\)60176-5](https://doi.org/10.1016/S1872-2067(14)60176-5)
- Ma, J.; Wang, C.; He, H. Transition metal doped cryptomelane-type manganese oxide catalysts for ozone decomposition. *Applied Catalysis B: Environmental*, 2017, 201, pp. 503–510. DOI: <https://doi.org/10.1016/j.apcatb.2016.08.050>
- Lian, Z.; Ma, J.; He, H. Decomposition of high-level ozone under high humidity over Mn-Fe catalyst: The influence of iron precursors. *Catalysis Communications*, 2015, 59, pp. 156–160. DOI: <https://doi.org/10.1016/j.catcom.2014.10.005>
- Rakitskaya, T.L.; Truba, A.S.; Raskola, L.A.; Ennan, A.A. Natural clinoptilolite modified with manganese(II) chloride in the reaction of ozone decomposition. *Chemistry, Physics, and Technology of Surface*, 2013, 4(3), pp. 297–304. (in Ukrainian). DOI: <https://doi.org/10.15407/hftp04.03>
- Rakitskaya, T.; Truba, A.; Radchenko, E.; Golub, A. Manganese(II) complexes with Schiff bases immobilized on nanosilica as catalysts of the reaction of ozone decomposition. *Nanoscale Research Letters*, 2015, 10, 472, pp. 1–9. DOI: <https://doi.org/10.1186/s11671-015-1179-6>
- Rakitskaya, T.L.; Ennan, A.A.; Granatyuk, I.V.; Bandurko, A.Yu.; Balavoine, G.G.A.; Geletii, Y.V.; Paina, V.Ya. Kinetics and mechanism of low-temperature ozone decomposition by Co-ions adsorbed on silica. *Catalysis Today*, 1999, 53(4), pp. 715–723. DOI: [https://doi.org/10.1016/S0920-5861\(99\)00158-3](https://doi.org/10.1016/S0920-5861(99)00158-3)
- Rakitskaya, T.L.; Bandurko, A.Yu.; Ennan, A.A.; Paina, V.Ya. Catalysts for sanitary air cleaning from ozone. *Catalysis Today*, 1999, 53(4), pp. 703–713. DOI: [https://doi.org/10.1016/S0920-5861\(99\)00157-1](https://doi.org/10.1016/S0920-5861(99)00157-1)

11. Zackay, V.F.; Rowe, D.R. A method of removing ozone from air. UK Application 2142324, 1985, No. 8415221.
12. Rump, H.; Kiesewetter, O. Sorption catalyst with small flow resistance for ozone decomposition in ventilating systems. FRG Application 10014485, 2001, No. 10014485.
13. Takeda Yakuhin Kogyo, K.K. Ozone Removal Method. Japan Application, 61-20329, 1986, No. 53-45712.
14. Rakitska, T.L.; Ennan, A.A.; Bandurko, O.Yu.; Paina, V.Ya.; Litvinska, V.V. Catalyst for ozone purification. Ukraine Patent 10368 A, 1996.
15. Boevski, I.; Genov, K.; Boevska, N.; Milenova, K.; Batakliiev, T.; Georgiev, V.; Nikolov, P.; Sarker, D.K. Low temperature ozone decomposition on Cu^{2+} , Zn^{2+} and Mn^{2+} exchanged clinoptilolite. Proceeding of the Bulgarian Academy of Sciences, 2011, 64(1), pp. 33–38.
<http://www.proceedings.bas.bg/>
16. Faming Zhuanli Shenqing. Catalytic material for decomposition of ozone at room temperature and its preparation method. China Application CN101357331, 2009, No. CN 200710044392.
17. Rakytskaya, T.L.; Bandurko, A.Yu.; Ennan, A.A.; Paina, V.Ya.; Litvinskaya, V.V. Low-temperature catalytic decomposition of ozone microconcentrations by carbon fibrous materials. Advances in Environmental Research, 2000, 3(4), pp. 472–487.
18. Rakitskaya, T.L.; Bandurko, A.Yu.; Ennan, A.A.; Paina, V.Ya.; Rakitskiy, A.S. Carbon-fibrous-material-supported base catalysts of ozone decomposition. Microporous and Mesoporous Materials, 2001, 43(2), pp. 153–160. DOI: [https://doi.org/10.1016/S1387-1811\(00\)00358-9](https://doi.org/10.1016/S1387-1811(00)00358-9)
19. Rakitskaya, T.L.; Truba, A.S.; Davtyan, A.S.; Berezina, L.V. Catalytic activity of basalt tuff anchored chloride complexes of Cu(II), Co(II), and Mn(II). Odesa National University Herald. Chemistry, 2010, 15(12), pp. 10–16. DOI: <https://doi.org/10.18524/2304-0947.2010.12.38444> (in Russian).
20. Centi, G.; Perathoner, S. Catalysis by layered materials: A review. Microporous and Mesoporous Materials, 2008, 107(1-2), pp. 3–15. DOI: <https://doi.org/10.1016/j.micromeso.2007.03.011>
21. Wan, D.; Li, W.; Wang, G.; Chen, K.; Lu, L.; Hu, Q. Adsorption and heterogeneous degradation of rhodamine B on the surface of magnetic bentonite material. Applied Surface Science, 2015, 349, pp. 988–996. DOI: <https://doi.org/10.1016/j.apsusc.2015.05.004>
22. Hong, R.; Guo, Z.; Gao, J.; Gu, C. Rapid degradation of atrazine by hydroxyl radical induced from montmorillonite templated subnano-sized zero-valent copper. Chemosphere, 2017, 180, pp. 335–342. DOI: <https://doi.org/10.1016/j.chemosphere.2017.04.025>
23. Carriazo, J.G.; Martinez, L.M.; Odriozola, J.A.; Moreno, S.; Molina, R.; Centeno, M.A. Gold supported on Fe, Ce, and Al pillared bentonites for CO oxidation reaction. Applied Catalysis B: Environmental, 2007, 72(1-2), pp. 157–165. DOI: <https://doi.org/10.1016/j.apcatb.2006.10.018>
24. Rakitskaya, T.L.; Kiose, T.A.; Zryutina, A.M.; Gladyshevskii, R.E.; Truba, A.S.; Vasylechko, V.O.; Demchenko, P.Yu.; Gryshouk, G.V.; Volkova, V.Ya. Solid-state catalysts based on bentonites and Pd(II)-Cu(II) complexes for low-temperature carbon monoxide oxidation. Solid State Phenomena, 2012, 200, pp. 299–304. DOI: <https://doi.org/10.4028/www.scientific.net/SSP.200.299>
25. Rakitskaya, T.; Dzhyga, G.; Kiose, T.; Volkova, V. Natural Nanobentonites as Supports in Palladium(II)-Copper(II) Catalysts for Carbon Monoxide Oxidation with Air Oxygen. Springer Proceedings in Physics: Springer: Cham, 2020, 247, pp. 141–157. DOI: https://doi.org/10.1007/978-3-030-52268-1_11
26. Rakitskaya, T.L.; Kiose, T.A.; Golubchik, K.O.; Dzhyga, G.M.; Ennan, A.A.; Volkova, V.Y. Catalytic compositions based on chlorides of d-metals and natural aluminosilicates for the low-temperature sulfur dioxide oxidation with air oxygen. Acta Physica Polonica A, 2018, 133(4), pp. 1074–1078. DOI: <https://doi.org/10.12693/APhysPolA.133.1074>
27. Rakytskaya, T.L.; Dzhyga, G.M.; Truba, A.S. Compositions based on palladium(II) and copper(II) compounds, halide ions, and bentonite for ozone decomposition. Odesa National University Herald. Chemistry, 2017, 22(2), pp. 6–14. DOI: [https://doi.org/10.18524/2304-0947.2017.2\(62\).102189](https://doi.org/10.18524/2304-0947.2017.2(62).102189) (in Ukrainian).
28. Rakitskaya, T.L.; Kiose, T.A.; Truba, A.S.; Ennan, A.A. Effect of water on activity and protective properties of catalysts used in respiratory protective equipment. IGI Global: Hershey, 2022, pp. 469–499. DOI: <https://doi.org/10.4018/978-1-7998-7356-3.ch021>
29. Rakitskaya, T.; Kiose, T.; Raskola, L. Synthetic zeolites modified with salts of transition metals in the reaction of chemisorption-catalytic oxidation of Sulphur dioxide by air oxygen. Chemistry Journal of Moldova, 2021, 16(2), pp. 91–101. DOI: <http://dx.doi.org/10.19261/cjm.2021.913>
30. Rakitskaya, T.; Truba, A.; Volkova, V.; Yaremov, P. Structural, Morphological, and Catalytic Properties of Cryptomelane. Springer Proceedings in Physics: Springer, Cham, 2020, 246, pp. 59–77. DOI: https://doi.org/10.1007/978-3-030-51905-6_6
31. Komadel, P.; Madejová, J. Acid activation of clay minerals. Developments in Clay Science, 2006, 1, pp. 263–287. DOI: [https://doi.org/10.1016/S1572-4352\(05\)01008-1](https://doi.org/10.1016/S1572-4352(05)01008-1)
32. Shashkova, I.L.; Ratko, A.I.; Milvit, N.V. Extraction of heavy metal ions from aqueous solutions using natural carbonate-containing terpels. Russian Journal of Applied Chemistry, 2000, 6(73), pp. 914–919. (in Russian).

33. Dorfman, Ya.A., Tyuleneva, L.V. Halide-ion catalysis of the oxidation reaction of hydrogen sulfide with ozone. Questions of kinetics and catalysis. Publishing house of the Ivanovo Institute of Chemical Technology: Ivanovo, 1976, pp. 38–41. (in Russian).
34. Michel, A.E.; Usher, C.R.; Grassian, V.H. Reactive uptake of ozone on mineral oxides and mineral dusts. *Atmospheric Environment*, 2003, 37(23), pp. 3201–3211. DOI: [https://doi.org/10.1016/S1352-2310\(03\)00319-4](https://doi.org/10.1016/S1352-2310(03)00319-4)
35. Rakitskaya, T.L.; Kiose, T.A.; Golubchik, K.O.; Ennan, A.A.; Volkova, V.Y. Acid-modified clinoptilolite as a support for palladium-copper complexes catalyzing carbon monoxide oxidation with air oxygen. *Chemistry Central Journal*, 2017, 11, 28, pp. 1–10. DOI: <https://doi.org/10.1186/s13065-017-0256-6>